Astron. Astrophys. 354, 802–814 (2000)

ASTRONOMY AND ASTROPHYSICS

Initial mass function in star formation complexes in galaxies

F. Sakhibov[1,2] **and M. Smirnov**[1]

[1] Institute of Astronomy, Russian Academy of Sciences, Pyatnitskaya str. 48, 109017 Moscow, Russia (fsakhibov@debitel.net)
[2] Insitute of Astrophysics, Tajik Academy of Sciences, Bukhoro str. 22, Dushanbe, 734042, Tajikistan

Received 30 November 1998 / Accepted 3 December 1999

Abstract. Star formation properties (slope α, upper mass limit M_{max} of IMF, age t) of 105 star formation complexes (SFCs) in 20 galaxies are estimated by inverting their observed integrated colours into parameters of star formation. Mass functions of individual star formation complexes are studied in three spirals, one irregular and one peculiar galaxy. The derived stellar initial mass functions (IMFs) in the studied galaxies are close to the Salpeter IMF with slopes $\alpha \in (-2.06 - -2.57)$. The calculated star formation rate (SFR) shows a burst of star formation in the peculiar colliding galaxy NGC 4038/39. The changes in star formation properties between different galaxies are related to the changes in individual SFCs mass functions and the correlation of the IMF of individual SFCs with their mass.

Key words: methods: data analysis – stars: formation – stars: luminosity function, mass function – ISM: H II regions – galaxies: star clusters – galaxies: stellar content

1. Introduction

In many investigations the individual star-forming complexes (SFCs), giant HII regions have been used to study the properties of star formation in galaxies (Bresolin & Kennicutt 1997; Mayya 1994; Terlevich & Melnick 1985; Vilchez & Pagel 1988). The stellar content of the SFCs may be probed by comparing observed spectra of stars plus gas with theoretically synthesised spectra, using an assumed IMF and SFR. The synthetic spectra are generally computed using stellar evolutionary tracks and model atmospheres: the evolutionary synthesis (Lequeux et al. 1981; Olofsson 1989; Leitherer & Heckman 1995; Mas-Hesse & Kunth 1991), or using a library of spectra of stars and stellar clusters: the population synthesis (Bica et al. 1990). The two methods are complementary and useful for confrontation of observations with the theories of stellar evolution, stellar atmospheres, and star formation. Synthesis of the observational parameters give the possibility to constrain the properties of star formation processes taking place in star forming regions. Plotting of theoretically computed evolutionary tracks on the observed two colours $U-B$ vs. $B-V$ diagram at fixed stellar IMF, SFR, chemical abundance Z, and age t for a given model of star formation is also a usual way of confrontation of observations with theory. This is applicable for the confrontation of theoretical tracks with observed colours of individual stars of stellar clusters. In case of external galaxies there are observed colours of star formation complexes not individual stars. The individual theoretical tracks show the variation of stellar spectra with age t at fixed IMF and Z of a given star formation model. Therefore the confrontation of observed colours of individual star formation complexes (SFCs) with individual model tracks (isochrones) on a whole range of variation of the model's parameters (IMF, t, Z) is difficult. The problem with similar methods of confrontation is that there are many free parameters leading to uncertainties in the results. These methods don't allow us to evaluate the theoretical parameters of star formation for individual SFCs and one can not detect variations of star formation in different star formation complexes in different galaxies.

To study the IMF in individual SFCs in external galaxies we need a method of analysis of their integrated emission fluxes, based on the research of integrated colours of models of stellar clusters (usually in $UBVR$ system). Previously we suggested with our colleagues (Myakutin et al. 1994; Sakhibov & Smirnov 1999a - hereafter paper II) a method for the comparison of the whole predicted and observed spectral energy distributions to set constraints on the stellar content, the method of inversion of integrated colours of individual SFC into star formation parameters (IMF and age of SFC t) in the frame of the evolutionary population synthesis models. Individual SFCs are very convenient to study star formation properties because of their intrinsic characteristics:

- the chemical abundances of gas and stars in a SFC are similar;
- the giant HII region is an ionisation bounded nebula, ionised by the stellar continuum below 912 Å emitted by the most massive stars in the SFC;
- there is a single mode IMF which approximates the mass spectrum of stars formed, with a slope α;
- the history of star formation in SFC is simple: there are no stars of second and next generations.

To avoid confusion we do like to make clear that under the term star formation complex (SFC) we mean a star forming

Send offprint requests to: F. Sakhibov

region observed in external galaxies as a giant extragalactic HII complex.

The plan of the paper is as follows: In Sect. 2 we present the evolutionary models of stellar population in star forming clusters and the underlying assumtions of the models. The method of simultaneous inversion of observed characteristics (colour indices of SFC) into intrinsic parameters of star formation processes (IMF, age, regime) is discussed in Sect. 3. The main input observable parameters (colour indices, chemical abundances, interstellar extinctions) are discussed in Sects. 4.1, 4.2, 4.3. In Sect. 4.4 we have discussed the accuracy of the method with the given sample of observational data. The derived star formation properties of the sample of 105 star forming regions are presented in Sect. 5. The derived mass spectra of star forming regions in the five nearby galaxies NGC 2403, NGC 2903, NGC 4038/39, NGC 4303, NGC 4449 are presented in Sect. 6. The integral stellar IMFs and star formation rates in these galaxies are disccused in Sect. 7. The results are summarised in Sect. 8, where some comments are also made on the emerging overall picture.

2. Evolutionary synthesis models

We used the model of stellar population in star forming complexes calculated by Piskunov & Myakutin (1996) - hereafter P&M. In this model the star formation in the SFC is described by a birth-rate function

$$b(m,t) = \frac{d^2N}{dmdt} \tag{1}$$

dN being the number of stars of mass m in the given mass interval dm and in the given time interval dt. A single generation aggregate is assumed in the SFC:

$$b(m,t) = f(m) \cdot r(t) \tag{2}$$

A power law form for the IMF was adopted $f \propto m^{\alpha}$, $m \in (M_{min}, M_{max})$, with M_{min}, M_{max} being the lower and upper mass limits of formed stars. Given $\alpha = -2.35$ we get the well known Salpeter IMF. Two models were adopted for the star formation rate (SFR):

$$r(t) = \begin{cases} \delta(t) \\ constant \end{cases} \tag{3}$$

The first branch corresponds to simultaneous star formation (hereafter the SSF model), and the second branch corresponds to infinite continuous star formation (the CSF model). To avoid an excessive number of parameters of the problem neither any particular period of star formation, nor any specific time dependence law for $r(t)$ were considered.

To predict fluxes emitted by stellar population of star forming complexes P&M construct a theoretical Hertzsprung-Russel diagram (HRD) of the SFC for the corresponding age and adopted set of star formation parameters and some other assumptions on star evolution details (e.g. mass loss).

Stellar evolutionary tracks aimed for the SFC theoretical HR diagram construction must fulfil a number of requirements:

- both early and advanced stages of evolution: $t \in (0.5, 100)$ Myr;
- both very massive and low mass models;
- various chemical compositions: $Z \in (0.002, 0.04)$;
- selected physical effects (such as mass loss).

Since no uniform grid of evolutionary tracks by the same author has been published in the literature, P&M were forced to compile a system of evolutionary tracks, satisfying the above conditions. They have constructed an extensive grid of evolutionary tracks (Myakutin 1992, 1995) by interpolation in and between original tables. The original tracks (Schaller et al. 1992, 1993; Charbonnel et al. 1993, 1993a, 1994) were reduced to the chemical composition grid adopted within the project.

To compare theoretical fluxes with observations some transformation scales are necessary. For transformations to UBV fluxes P&M used scales of bolometric corrections and Johnson photometry colours, published by Schmidt-Kaler (1982). These tables represent the most complete set of scales since they include data for a wide variety of spectral classes (from O to M stars) and luminosity classes (V, III, I). An error introduced by this specific choice was evaluated with the help of test calculations of integrated colours using other independent scales published in the literature (Johnson 1966; Sagar et al. 1986). P&M found typical errors of integrated colours $U-B$, $B-V$ of a young SFCs ($\log(t) < 7.5$) arising from using different scales to be in the order of 0.01^m which is much smaller than the errors of the observed colours.

To calculate fluxes of Lyman continuum photons (Lc) P&M used a calibration scale based on NLTE atmosphere models (Avedisova 1979). The calibration is valid for the range of $Teff = 15000K - 50000K$ and the range of a gravitational acceleration $\log(g) = 3.5, 4.0$. The blanketing corrections were taken into account.

Theoretical stellar content of SFC had been represented in the form of four dimensional functions of colour indices $U-B$, $B-V$, $V-R$, LCI as a function of star formation parameters: high-mass end M_{max} and slope α of IMF, age t of SFC, and chemical abundance Z:

$$\begin{array}{l} (U-B) = f_1(\alpha, M_{max}, t, Z) \\ (B-V) = f_2(\alpha, M_{max}, t, Z) \\ (V-R) = f_3(\alpha, M_{max}, t, Z) \\ LCI = f_4(\alpha, M_{max}, t, Z) \end{array} \tag{4}$$

LCI is the Lyman continuum index: $LCI = 2 - log[(I_{H_\alpha+NII}/I_B]$, where the emission line intensity of $I_{H_\alpha+NII}$ is in units $ergs/(s \cdot cm^2)$ and continuum flux intensity I_B is in units $ergs/(s \cdot cm^2 \cdot$Å). As we are dealing with ionisation bound star formation regions (Case B), the ionising continuum Lc, comprising all the photons with $\lambda < 912$ Å, can be computed from the known value of the H_α intensity. A detailed description about how the colour indices were computed for a broad range of ages can be found in the paper by P&M.

In Fig. 1 the area covered by the theoretical models on $(U-B)$ vs. $(B-V)$ diagram (inner box) is displayed. The range of slope α variation is $(-0.35, -4.35)$; the range of upper mass limit M_{max} is $(30M_\odot, 120M_\odot)$; the range of $\log(t)$

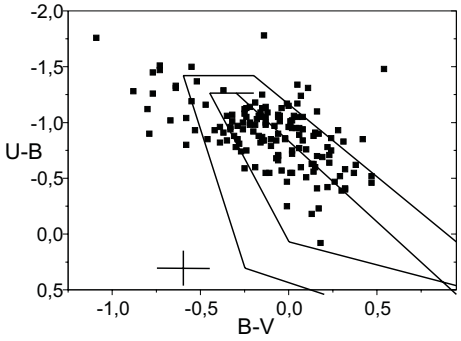

Fig. 1. Area of theoretical model on the two colours diagram (inner box).

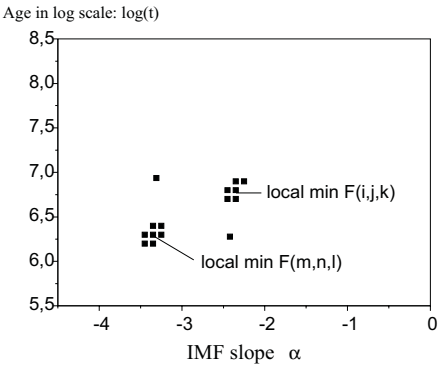

Fig. 2. A $\alpha - \log(t)$ plane of the SFC model. The local minima $F_{i,jk}$ is defined as the value of $F_{i,jk}$, which is lower than the values of function F in all 8 neighbouring nodes.

is $(5.7, 8.3)$; the range of SFR models is (SSF-model, CSF - model). The outer box traces the area corresponding to one standard deviation of colour indices 0.25^m. The points are the observed colours of individual SFCs in 16 galaxies which will be discussed below. The objects outside the outer box lie within 3 standard deviations.

3. Method

3.1. Inversion of colour indices into star formation parameters

The models of stellar population in star forming complexes are presented in the form of a grid of colour indices for a broad range of variation of parameters $\alpha(i)$, $t(j)$, $M_{max}(k)$ (see Sect. 2). Here indexes i, j, k are number of rows and columns in a three dimensional grid of colour indices. The table steps of slope α variation is $h_\alpha = -0.1$; of M_{max} parameter variation is $h_{Mmax} = 30 M_\odot$; of $\log(t)$ parameter variation is $h_{\log(t)} = 0.2$. A two dimensional cut of model in plane $\alpha - \log(t)$ is shown in Fig. 2, at fixed M_{max} and Z. Each point on the $\alpha - \log(t)$ plane corresponds to a set of predicted colour indices $(U-B)^{i,j,k}_{tab}$, $(B-V)^{i,j,k}_{tab}$, $(V-R)^{i,j,k}_{tab}$, $LCI^{i,j,k}_{tab}$.

The procedure for finding the values of IMF parameters α, M_{max} and age t, which are appropriate for the set of observed colours (finding the roots of the problem) can be subdivided into three steps.

The first step is to compute a special function $F(\alpha, M_{max}, t, U, B, V, R, Lc)$. For the given observational data set of colours $(U-B)_{obs}$, $(B-V)_{obs}$, $(V-R)_{obs}$, LCI_{obs}, and chemical abundance Z the following $(O-C)$ parameters (observation minus computation) have been defined for each node $(\alpha(i), \log(t(j)), M_{max}(k))$ of model's grid:

$$\begin{array}{l} (O-C)^{i,j,k}_1 = (U-B)_{obs} - (U-B)^{i,j,k}_{tab} \\ (O-C)^{i,j,k}_2 = (B-V)_{obs} - (B-V)^{i,j,k}_{tab} \\ (O-C)^{i,j,k}_3 = (V-R)_{obs} - (V-R)^{i,j,k}_{tab} \\ (O-C)^{i,j,k}_4 = LCI_{obs} - LCI^{i,j,k}_{tab} \end{array} \quad (5)$$

For every grid node (i, j, k) we calculated the value of function F:

$$F_{i,j,k} = \sqrt{\sum_{l=1}^{4} [(O-C)^{i,j,k}_l]^2} \quad (6)$$

The second step is to build a linear approximation of the theoretical model (at given Z) assuming a multiple regression model between star formation parameters α, M_{max}, t and colour indices:

$$\begin{array}{l} \alpha - a_2 M_{max} - a_3 t = a_1 + a_4(U-B) + a_5(B-V) + \\ \quad + a_6(V-R) + a_7 LCI + \epsilon \end{array} \quad (7)$$

where parameters $a_1, a_2, \cdot, \cdot, \cdot, a_7$ are estimated by the least square method procedure, the random variable ϵ is an error term that accounts for the variability in α, M_{max}, t that cannot be explained by the linear relation. A correlation coefficient $r = 0.90$ shows that the fit provided by the estimated regression equation appears to be good.

The third step is searching for the roots of the problem. We searched for the grid node table in which the following three conditions are valid simultaneously:

(i) modules of the (O-C) differences are less than the accuracy of the observational data:

$$\begin{array}{ll} \mid (O-C)^{i,j,k}_1 \mid \leq \sigma_{U-B} & \mid (O-C)^{i,j,k}_2 \mid \leq \sigma_{B-V} \\ \mid (O-C)^{i,j,k}_3 \mid \leq \sigma_{V-R} & \mid (O-C)^{i,j,k}_4 \mid \leq \sigma_{LCI} \end{array} \quad (8)$$

(ii) function $F_{i,j,k}$ has deepest local minimum, the local minima of function F in the particular grid node (i, j, k) is defined as the value of $F_{i,j,k}$, which is lower than the values of function F in all 8 neighbouring nodes:

$$\begin{array}{l} F_{i,j,k} < F_{i-1,j-1,k};\ F_{i,j,k} < F_{i,j-1,k};\ F_{i,j,k} < F_{i+1,j-1,k}; \\ \quad F_{i,j,k} < F_{i-1,j,k}; \quad F_{i,j,k} < F_{i+1,j,k}; \\ F_{i,j,k} < F_{i-1,j+1,k};\ F_{i,j,k} < F_{i,j+1,k};\ F_{i,j,k} < F_{i+1,j+1,k} \end{array} \quad (9)$$

(iii) the difference between the modules of left and right parts of the estimated regression Eq. (7) is less than the standard deviation σ of the error term ϵ in the regression model:

$$\begin{array}{l} \mid \alpha - a_2 M_{max} - a_3 t \mid - \mid a_1 + a_4(U-B) + \\ \quad + a_5(B-V) + a_6(V-R) + a_7 LCI \mid < \sigma \end{array} \quad (10)$$

In case where there is a single node of model's grid $(\alpha(i), \log(t(j)), M_{max}(k))$, where all three above mentioned conditions are valid, we accepted corresponding values $\alpha =$

Table 1. The individual accuracy of different authors and systems.

Author/System	σ_{U-B}	σ_{B-V}	σ_{V-R}	σ_{LCI}
Shapovalova 1971	0.17	0.16		
CrAO 1	0.13	0.19		0.10
CrAO 2	0.13	0.50	$<$0.15	
Shahbazian 1970	0.09	0.16		
Mayya 1994		0.22	$<$0.15	0.09
McCall et al. 1985	0.11	0.22		0.16
Khachikian & Sahakian, 1970		0.40		

$\alpha(i)$, $t = t(j)$, $M_{max} = M_{max}(k)$ as roots of the problem for the given set of observed colours and metallicity of individual SFC. In case where there are two or more nodes with $F_{i,j,k} \approx F_{m,n,l}$ we assumed that there is not a unique solution for a given SFC. We used grids for both models: the simultaneous star formation model (SSF) and the infinite continuous star formation model (CSF).

4. Observational data

4.1. Colour indices

In our previous paper (Sakhibov & Smirnov 1999, hereafter paper I) we collected available U, B, V, R, H_α and multicolour photometry data for the 836 extragalactic HII-regions in 49 galaxies. There are many photometry observations of extragalactic HII regions carried out on different telescopes, and using different techniques. Authors used the standard $UBVR$ system as well as some special narrow and middle band photometry systems:

(i) McCall et al. (1985) used the photometry system with 100 Å pass bands centred on 4036 Å and 4785 Å and 200 Å pass band centred on 5445 Å. The colour of blue spectra is represented by $m_\nu(4036) - m_\nu(4785)$; the colour of yellow spectra is characterised by $m_{nu}(4785) - m_{nu}(5445)$. Let us mark this photometry system as MRS.

(ii) Pronik and her colleagues from Crimean Astrophysical Observatory (Pronik & Chuvaev 1967, 1969, 1971, 1972; Pronik 1972; Grigorieva 1976, 1979, 1980; Dobrodiy & Pronik 1979) used 200 Å pass bands centred on continuum emission 3600, 4680, 5280, 6090 and 7400 Å, and 160 Å pass bands centred on emission lines 3730, 5060, 6600 Å (hereafter CrAO photometry system). The colour of blue spectra is represented by ratio I_{3600}/I_{4680}. The ratios I_{4680}/I_{5280} and I_{4680}/I_{6090} characterise the yellow spectra. The colour of red spectra is characterised by ratio I_{5280}/I_{7400}. The system based on the ratios I_{3730}/I_{4680} and I_{4680}/I_{6090} is marked as CrAO 1; the system based on the ratios I_{3600}/I_{4680}, I_{4680}/I_{5280} and I_{5280}/I_{7400} is marked as CrAO 2

(iii) D'Odorico et al. (1983) derived the B and V magnitudes from monochromatic fluxes at 4450 Å and 5500 Å respectively.

We have converted the monochromatic intensity ratios into $U-B, B-V, V-R$ colour and LCI indices using the calibration developed in paper I. We identified all HII regions (SFCs) observed by different authors and used the overlaps of the different samples to estimate the accuracy of each individual author. This technique is similar to the procedure for the estimation of the accuracy of the method discussed below in Sect. 4.4. The individual accuracy of different authors is listed in Table 1. The values of σ_{V-R} are upper limits of the accuracy. We did not consider $UBVR$ and H_α photometry of 276 SFCs in 10 galaxies published by Bresolin & Kennicutt in 1997, when the paper I was completed. We also note that there is no overlap between our sample of 836 SFCs with above mentioned 276.

4.2. Chemical abundance

We have used spectral observations data of SFCs in 39 galaxies (Zaritsky et al. 1994) to account for interstellar light extinction and to calculate the chemical abundance of SFCs. We have completed the list by Zaritsky et al. (1994) with published spectral observation in another 10 galaxies (paper II). We identified the overlaps of different samples of spectral observations of SFCs and estimated the errors of individual authors by the technique described in Sect. 4.4. To characterise the accuracy of individual observations we classified different observational data samples according to their error's estimations:

- class I observation of $[OIII]/H_\beta$ ratio has a standard error $\sigma < 0.05$ (in logarithmic scale of intensity);
- class II observation of $[OIII]/H_\beta$ ratio has a standard error $0.05 < \sigma \leq 0.10$;
- class III observation of $[OIII]/H_\beta$ ratio has a standard error $0.10 < \sigma \leq 0.20$;
- class IV observation of $[OIII]/H_\beta$ ratio has a standard error $0.20 < \sigma \leq 0.50$;

The observations of $[NII]/H_\alpha$ ratio are subdivided into following classes:

- class I observation has a standard error $\sigma < 0.10$;
- class II observation has a standard error $0.10 < \sigma \leq 0.15$;
- class III observation has a standard error $0.15 < \sigma \leq 0.20$;
- class IV observation has a standard error $0.20 < \sigma \leq 0.50$;

To estimate the chemical abundance $Z/Z_\odot$ we used semiempirical relations between line intensity ratios and metallicities studied in our previous paper (Sakhibov & Smirnov 1990). We accounted for the class (accuracy) of metallicity observation in our estimation of chemical abundance Z. The variation of Z estimations of SFCs is about 50%.

4.3. Interstellar extinction

Estimates and corrections for the interstellar extinction of light are required in the studied SFCs. The observed Balmer decrement usually provides the estimates of the interstellar extinction. Direct use of these corrections for interstellar reddening in the studied SFCs gives unreasonable blue colours. This is probably a result of the overestimation of the interstellar reddening. This effect may be caused by the difference between gas emission extinction and reddening of stars in SFC. Caplan & Deharveng

(1986) studied the features of extinction of gas emission lines (Balmer decrement) and reddening of stars in HII regions in the Large Magellanic Cloud. Extinction of gas emission is systematically greater than that of stars in the same HII region. Mas-Hesse & Kunth (1991, 1999) found a significant discrepancy between the extinction measured on the stellar continuum and the reddening derived from the ratio of the Balmer emission lines in 17 star forming regions in irregular and compact galaxies. Bidimensional spectroscopy of star forming regions in the centre of NGC 4214 (Maiz-Apellaniz et al. 1998) shows the spatial decoupling between gas, stars and dust clouds. The dust appears concentrated at the boundaries of the ionised region, affecting mainly the nebular emission lines, while the stellar continuum itself is located in a region relatively free of dust and gas. This decoupling may explain the differences in extinction between the stellar continuum and the emission lines. Therefore, we suggest that the application of gas extinction A_v^{gas} (Balmer extinction) to extinction correction of stars photometry observations is not quite right. There is no theoretical model of dust spatial distribution in SFCs to derive the difference between the light extinction of gas and stars. In our previous paper (Sakhibov & Smirnov 1995) the discrepancies between the extinction of gas emission and that of the starlight in giant HII regions - star forming complexes in the galaxies M33, LMC and NGC 2403 - were investigated. We derived an empirical relation between the starlight extinction A_v^* and that of the gas A_v^{gas} emission in giant HII regions - star forming complexes:

$$A_v^* = (1-b)\cdot A_v^{Gal} + b\cdot A_v^{gas} \tag{11}$$

where coefficient b = 0.65 and A_v^{Gal} is the light extinction in the Galaxy. The last formula is derived under the assumption that gas emission extinctions consist of extinction in SFC and that in Galaxy: $A_v^{gas} = A_v^{gas}(SFC) + A_v^{gas}(Gal)$. In the case of no gas extinction in SFC, but strong Galactic absorption, we would get $A_v^{gas} = A_v^{gas}(Gal)$ and in the continuum $A_v^* = A_v^{Gal}$.

Since this relation between the extinction of starlight and that of the gas emission was derived from the observations of SFCs in different type of galaxies, we assumed that relation can be used in cases of other galaxies too.

The estimations of light extinction A_v^* are subdivided into 3 classes:

- class I estimation has a standard error $\sigma_{A_v^*} < 0.30^m$ (magnitudes);
- class II estimation has a standard error $0.30^m < \sigma_{A_v^*} \leq 0.50^m$;
- class III estimation has a standard error $\sigma_{A_v^*} > 0.50^m$.

To correct for light extinction we have used class I and class II estimations of A_v^*. The effect of the uncertainty of A_v^* on the result is accounted for in the first step of the procedure of inversion of colour indices into star formation parameters (see Sect. 3.1). The standard errors for the colour indices (used in Sect. 3.1) account for the uncertainty of extinction. For example the standard error for the $(U-B)$ is calculated as

$$\sigma_{U-B} = \sqrt{\sigma^2_{U-B}(obs) + [(E_U - E_B)\cdot \sigma_{A_v^*}]^2} \tag{12}$$

where E_U is the extinction coefficient for the U band, E_B is the extinction coefficient for the B band. The A_v^* accuracy $\sigma \approx 0.50^m$ increases the standard error of observed colour indices up to 0.25^m. The method's accuracy with the given sample of observational data is discussed in Sect. 4.4.

4.4. Accuracy of the method

To derive three parameters α, M_{max}, t, three observed colours are enough at observationally derived and fixed chemical abundance Z. A set of four colour indices $(U-B)_{obs}$, $(B-V)_{obs}$, $(V-R)_{obs}$, LCI_{obs}, provide us with five samples of input data, hence with five independent estimates of star formation parameters for given SFC:

1. $(U-B), (B-V), (V-R), LCI$
2. $(U-B), (B-V), LCI$
3. $(B-V), (V-R), LCI$
4. $(U-B), (V-R), LCI$
5. $(U-B), (B-V), (V-R)$

For example there are 5 estimates of parameter $\alpha(\alpha_1, \alpha_2, \alpha_3, \alpha_4, \alpha_5)$ derived for every given SFC. The number of SFCs is equal to N. Let $\Delta_{12}(i)$ be the difference between the two estimations of the parameter α for given SFC:

$$\Delta_{12}(i) = \alpha_1(i) - \alpha_2(i), \quad (i = 1, 2, \cdot, \cdot, \cdot, N) \tag{13}$$

Since the expected value (mean) of a random variable $\Delta_{12}(i)$ is equal to zero, the standard deviation can be calculated as

$$\sigma_{12}^2 = \frac{\sum_{i=1}^{N} [\Delta_{12}(i)]^2}{N-1} \tag{14}$$

Let σ_1 and σ_2 be standard deviations of the estimations of $\alpha_1(i)$ and $\alpha_2(i)$ correspondingly, derived for N SFCs $(i = 1, 2, \cdot, \cdot, \cdot, N)$. Since these two estimates are independent we can write that

$$\sigma_1^2 + \sigma_2^2 = \sigma_{12}^2 \tag{15}$$

The calculated values of σ_{12}^2, σ_{13}^2, σ_{14}^2, σ_{15}^2, σ_{23}^2, σ_{24}^2, σ_{25}^2, σ_{34}^2, σ_{35}^2, σ_{45}^2 provide with ten equations to derive five unknown values σ_1, σ_2, σ_3, σ_4, σ_5 of the estimations of parameter α from the five different sets of input data (see Table 2). The standard errors of the estimations of M_{max} and $\log(t)$ are derived in a similar way and are presented in Table 2.

The method's accuracy with the given sample of observational data ($\sigma_{obs} = 0.15^m - 0.28^m$ and $\sigma_z/Z = 50\%$) was accepted as mean value of estimated σ_1, σ_2, σ_3, σ_4, σ_5 for the SF parameters α, M_{max}, t: $\sigma_\alpha = 0.51 \pm 0.03$, $\sigma_{M_{max}} = (33 \pm 2) M_\odot$, $\sigma_{log(t)} = 0.29 \pm 0.03$.

5. IMF, age and mass of SFC derived from colour indices

To derive three parameters α, M_{max}, t we need at least three colours corrected for light extinction and chemical abundance Z of individual SFC. There are 180 SFCs from the list in paper I with known three or four colours, light extinction and Z.

Table 2. Standard deviations of the estimations of star formation parameters α, M_{max}, t estimated for the five sets of input data.

	$U-B$, $B-V$, $V-R$, LCI	$U-B$, $B-V$, LCI	$U-B$, $V-R$, LCI	$B-V$, $V-R$, LCI	$U-B$, $B-V$, $V-R$
	σ_1	σ_2	σ_3	σ_4	σ_5
σ_{Mmax} $[M_\odot]$	39	32	31	33	31
σ_α	0.46	0.43	0.55	0.53	0.58
$\sigma_{log(t)}$	0.23	0.35	0.23	0.26	0.36

The confrontation of the observed colour indices of these 180 SFCs with predicted model's colour indices using the method discussed in Sect. 3.1 provides us with estimations of the IMF slope α, upper mass limit M_{max}, and age t of 113 SFCs in 22 spiral and irregular galaxies (Table 3). In the case of the other 67 SFCs with known colour indices, the solution is not unique. To account for the number of ionising photons, which do not contribute to the ionisation process (Smith et al. 1978; Mezger 1978), we have assumed that 30% - 40% of the photons below 912 Å in some SFCs are directly absorbed by dust.

5.1. *Significance of the estimated IMF parameters*

Observed absolute magnitudes of studied SFCs lie in a broad interval from -5^m to -19^m. This means that the number of stars in the individual SFC also changes in a broad interval from 50 to $5\cdot10^8$. From the observed absolute magnitude $M_B(obs)$ of SFC one can calculate the initial B luminosity L_{SFC} for the moment of the onset of star formation process ($t = 0$ year), using the derived IMF, age t and the evolutionary model discussed in Sect. 2. Relation between the initial absolute magnitudes and observed ones is shown in Fig. 3. Circles correspond to the continuous star formation process, squares correspond to the starburst star formation. In the case of starburst episode (SSF model), the linear regression equation between the initial absolute magnitude $M_B(initial)$ and the observed one $M_B(obs)$ with the coefficient of correlation r = 0.96 appears to be good:

$$M_B(initial) = -(0.33 \pm 0.70) + (1.04 \pm 0.04) M_B(obs) \quad (16)$$

In the case of continuous star formation the coefficient of correlation is $r = 0.89$:

$$M_B(initial) = (0.12 \pm 1.12) + (1.34 \pm 0.09) M_B(obs) \quad (17)$$

The number of stars formed in SFC at the onset of star formation can be estimated from the initial luminosity L_{SFC} by the solution of the system of two equations written below:

$$N_{stars\,in\,SFC} = A \int_{M_{min}}^{M_{max}} m^\alpha dm \quad (18)$$

$$L_{SFC} = A \int_{M_{min}}^{M_{max}} L^*(m) \cdot m^\alpha dm \quad (19)$$

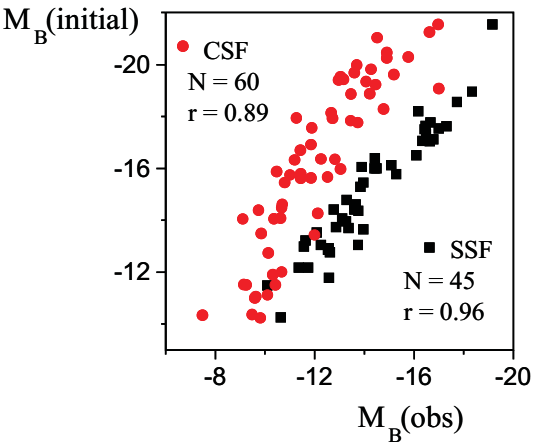

Fig. 3. Observed absolute magnitudes of 105 SFCs vs. initial ones computed using derived ages, IMFs and regimes of star formation in the frame of the evolutionary model.

where $L^*(m)$ is the known function of stellar luminosity in B band (Allen 1973), m is stellar mass, α is the estimated IMF slope, M_{max} is the estimated IMF upper mass limit, M_{min} is the IMF low mass limit, assumed to be equal to $0.1M_\odot$. The normalising constant A estimated from Eq. (19) corresponded to the IMF, since the L_{SFC} is the initial luminosity of SFC. The number $N_{stars\,in\,SFC}$ corresponds to stars within the IMF boundaries (M_{min}, M_{max} and corresponding slope α) at moment of the onset of star formation ($t = 0$).

So far as the IMF is a statistical function of the distribution of stellar masses, a small number of stars in SFC provides a poor estimate of the IMF parameters. In SFCs with IMF flatter than $\alpha = -3.32$ at a given function of stellar luminosity $L^*(m)$, 80% of the luminosity L_B is provided by stars with mass $m > 4M_\odot$. The factor of variation of input photometry data is about $15\%-20\%$. Therefore the accuracy of 20% of input photometry data can yield a significant value of the α estimation only for the high mass part of IMF ($m > 4M_\odot$). Since few massive stars can provide more than 80% of low luminosity SFC with a flat IMF, the estimate of the upper limit of IMF M_{max} cannot be significant. The estimate of M_{max} can be assumed as significant when the possible number of stars with a mass greater than the upper limit of IMF $N_p(m > M_{max}) \geq 1$. In the opposite case the estimates of IMF parameters for given SFC can be a result of a random fluctuation in stellar mass distribution. We accepted the possible number of stars in mass interval $(M_{max}, M_{max} + 30M_\odot)$

$$N_p = A \int_{M_{min}}^{M_{max}+30M_\odot} m^\alpha dm \geq 3 \quad (20)$$

as a criteria of the significance of the estimation of slope α and upper mass limit M_{max} of IMF in an individual SFC. Using this criteria we have selected 105 of the 113 studied SFCs in 20 galaxies with significant estimates of IMF parameters.

Table 3. The galaxy sample with studied 113 star forming regions. Numerical index T on the stage of Hubble sequence and numerical index LC on the stage of David Dunlap Observatory luminosity class indicated in Table 3 are taken from de Vaucouleurs et al. (1976).

NGC	Hubble type	T type index	LC luminosity class index	Number of SFCs	NGC	Hubble type	T type index	LC luminosity class index	Number of SFCs
628	Sc	5	1	4	4303	Sbc	4	1	17
1365	SBb	3	2	8	4321	Sbc	4	1	5
1566	Sbc	4	2	1	4449	Ir	10	5	9
2403	Scd	6	5	8	5055	Sb	4	3	2
2903	Sbc	4	2	8	5194	Sc	4	1	8
2997	Sc	5	1	3	5253		0	6	1
3184	Scd	6	3	4	5457	Sc	6	1	1
3351	SBb	3	3	3	6946	Scd	6	1	5
4038/39	Peculiar	9	1	8	7793	Sd	7	7	1
4088	Sbc	4	2	2	Ic342	Sd	6	2	4
4254	Sc	5	1	5	LMC	SBm	10	6	6

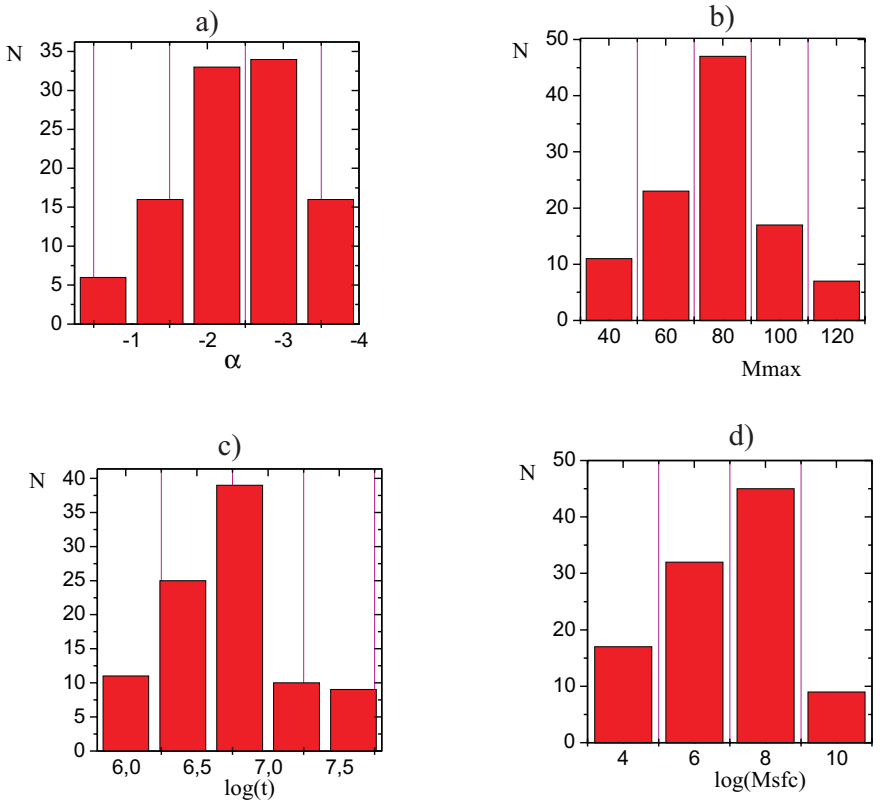

Fig. 4a – d. Histograms: **a** of the IMF slope α, **b** of the upper mass limit of IMF M_{max}, **c** of the age t, **d** of the mass M_{SFC} distribution of 105 SFCs in 20 galaxies.

5.2. Distribution of the estimated star formation properties of SFCs

Derived estimates of α show a broad range of the variation of the IMF slope in 105 SFCs, $\alpha \in (-0.50, -4.00)$, with a mean value $\alpha \approx -2.42$ close to Salpeter IMF. A normal approximation to the derived distribution (Fig. 4a) of α has a standard deviation $\sigma_\alpha(obs) = 0.9$ greater than the standard error of the method $\sigma_\alpha = 0.51$. So the derived distribution of slope in studied SFCs is meaningful. The IMF slopes constrained by Mas-Hesse & Kunth (1999) for a sample of 17 star forming regions (mostly irregular and blue dwarf galaxies) to the range from -1 up to -3, with a mean value between Salpeter one ($\alpha = -2.35$) and Scalo (1986), $\alpha = -2.85$.

Estimations of the upper limit of IMF M_{max} covering the grid's interval $(30M_\odot, 120M_\odot)$ show a distribution (Fig. 4b) with mean value $74M_\odot$ and standard deviation of the normal approximation $\sigma_{Mmax}(obs) = 20M_\odot$, which is less than the standard error of the method $\sigma_{Mmax} = 33M_\odot$.

Age estimations of SFCs show a range from $\log(t) = 5.9$ to $\log(t) = 8.0$ (Fig. 4c). Relatively old SFCs are experiencing an infinite continuous star formation (the CSF model). The mean value of age estimations is about 7 Myr. The standard deviation $\sigma_{log(t)}(obs) = 0.55$ is greater than the standard error

of the method $\sigma_{log(t)} = 0.29$. The age distribution of 45 SFCs with simultaneous star formation (SSF model) shows a mean age $(4.5^{+4.5}_{-2.5})$ Myr, while that of SFCs with infinite continuous star formation (CSF model) shows a mean age (10^{+30}_{-8}) Myr. The spread in the age of the 14 intense starbursts in irregular and compact galaxies estimated by Mas-Hesse & Kunth (1999) is more narrow (2.5 - 6.5 Myrs). It should be noted that instantaneous star formation regime (SSF model) is preferred by Mas-Hesse & Kunth (1999) and their sample is biased toward very young bursts. There are strong constraints in 3 objects by Mas-Hesse & Kunth (1999) toward constant star formation rates (CSF model) during at least 10 - 15 Myr.

5.3. Mass of the stellar population in SFC

Knowing the the IMF slope α, upper mass limit M_{max} and initial luminosity L_{SFC} of star forming regions allows us to estimate a total amount of gas transformed into stars in SFC at the onset of star formation:

$$M_{SFC} = A \int_{M_{min}}^{M_{max}} m \cdot m^{\alpha} dm \qquad (21)$$

where m is stellar mass. The normalising constant A is estimated from the initial luminosity L_{SFC}, derived slope and upper mass limit of IMF by Eq. (19). This mass corresponds to stars within the IMF boundaries (M_{min}, M_{max}). In Fig. 4d the histogram of mass estimations frequency distribution is shown. The range of mass variation of SFCs is very large $(10^3 M_\odot, 10^{11} M_\odot)$, similar to the interval of observed brightness variation from -5^m to -19^m. The range of mass of the 17 star forming regions derived by Mas-Hesse & Kunth (1999) is from $500 M_\odot$ up to $10^8 M_\odot$. Mas-Hesse & Kunth (1999) have estimated mass of star forming region within the upper part of IMF from $2M_\odot$ up to $120 M_\odot$. The mass distribution of SFCs has a mean $log(M_{SFC}) = 6.99$, standard deviation $\sigma_{Msfc} = 1.76$ in a logarithmic scale.

Throughout the calculations a lower mass limit $M_{min} = 0.1 M_\odot$ is adopted for the IMF. The calculated masses of the largest SFCs are so high that these super massive complexes are gravitational bound objects. In case of adopted $M_{min} > 0.1 M_\odot$ the masses of larger SFCs are not so high and these SFCs would not be gravitational bound objects any longer. As was noted above, the IMF parameters estimated from observed colours of SFC are related to the upper part of the IMF $(m > 4 M_\odot)$. The IMF slope for low mass stars may be different. If the low end of the IMF has a flatter slope than the upper end of the IMF, the estimates of mass SFCs would be much lower even when $M_{min} < 0.1 M_\odot$.

In paper II we estimated a linear regression equation between α and stellar mass of star forming region M_{SFC}:

$$\alpha = (0.05 \pm 0.22) - (0.35 \pm 0.03) \log(M_{SFC}) \qquad (22)$$

Table 4. List of the selected galaxies with a complete sample of SFCs with known B magnitudes.

Galaxy	Distance (Mpc)	Number of SFCs	Limit in magnitudes of the statistics completeness	Number of SFCs with derived IMF,age
2403	3.2	41	$M_B < -7^m$	7
2903	7.5	36	$M_B < -11^m$	8
4038/39	18.0	22	$M_B < -13^m$	7
4303	18.0	56	$M_B < -12^m$	16
4449	4.3	85	$M_B < -10^m$	9

where correlation coefficient $r = 0.75$. To predict the values of M_{SFC} and α from the observed $M_B(obs)$, we have estimated the linear regression Eqs. (23) and (24) written below:

$$\alpha = (-1.79 \pm 0.11) - (0.73 \pm 0.02) \log(M_{SFC}) - \\ - (0.28 \pm 0.01) M_B \qquad (23)$$

where M_B is the initial absolute magnitude of SFC at moment $t = 0$, computed from the observed absolute magnitude, derived IMF and age t using the evolutionary model. The correlation coefficient here is $r = 0.96$. The Eq. (23) is shown in Fig. 5a as a relation between the linear combination of two variables α and M_{SFC} $(\gamma = \alpha + 0.73 \cdot log(M_{SFC}))$ and initial luminosity M_B. The broadness of strip in Fig. 5b is caused by the spread of slope α in individual SFCs.

$$\log(M_{SFC}) = (-2.43 \pm 1.31) - (0.60 \pm 0.04) M_B \qquad (24)$$

6. Mass functions of SFCs in studied galaxies

To calculate the integral IMF for a given galaxy we have to know the IMF of every individual SFC in this galaxy. The studied 105 SFCs are distributed in 20 galaxies, therefore the sample of SFCs in each studied galaxy is incomplete. To estimate the slope α of IMF in an individual SFC we can use the semiempirical relations (23), (24) between initial luminosity M_B and slope α and mass M_{SFC} of star forming region plus theoretical relations (19), (21). Initial luminosity M_B can be estimated from the observed one from the empirical relations (16) and (17) discussed in Sect. 5.1. We have created a special procedure to solve the Eqs. (16, 17, 19, 21, 23, 24) system and to constrain IMF (slope α, M_{max}, normalising constant A) and mass from observed luminosity of SFC.

Knowing the observed B magnitudes of star forming region provides with an estimation of the slope α of its IMF and initial mass M_{SFC} within adopted evolutionary model. In other words, to get a complete sample of SFCs in a selected galaxy with the estimated IMF slope α, we need a complete survey of luminosity of star forming regions in this galaxy. We selected five galaxies from Table 3 with a complete sample of SFCs with observed B magnitudes and known light extinction (Table 4). The statistics in each galaxy are complete down to a limit in magnitudes indicated in Table 4. Luminosity of SFCs are taken

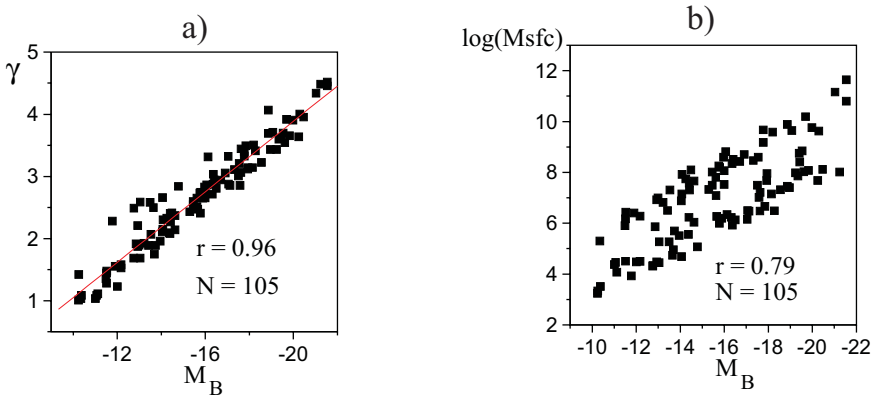

Fig. 5. a Scatter diagram of initial luminosity M_B and linear combination of α and M_{SFC}: $\gamma = \alpha + 0.73 \cdot log(M_{SFC})$. **b** Scatter diagram of initial luminosity M_B and initial mass M_{SFC}.

Table 5. The characteristics of mass, luminosity and size distributions in the selected galaxies.

Galaxy NGC	Mass function slope b		range of M_{SFC} $[logM_\odot]$		Mean mass of SFCs $[logM_\odot]$		range observed M_B [mag]	Mean M_B of SFCs [mag]	range of sizes l [pc]	Mean size of SFCs [pc]
	SSF	CSF	SSF	CSF	SSF	CSF				
2403	-0.46	-0.40	3.9 - 7.3	3.9 - 8.0	5.0	5.3	-5.2 - -14.2	-8.5	15 - 330	50
2903	-0.63	-0.42	3.9 - 8.2	4.5 - 9.2	5.7	6.9	-9.3 - -15.2	-11.7	70 - 360	170
4038/39	-0.38	-0.38	5.0 - 9.1	6.4 - 9.2	6.9	8.0	-12.6 - -17.3	-14.6	300 - 560	425
4303	-0.53	-0.46	4.4 - 7.9	5.7 - 9.9	6.2	7.5	-11.1 - -16.5	-13.3	130 - 930	385
4449	-0.48	-0.46	3.7 - 7.4	4.0 - 9.5	5.6	6.3	-8.1 - -16.5	-11.2	40 - 300	99

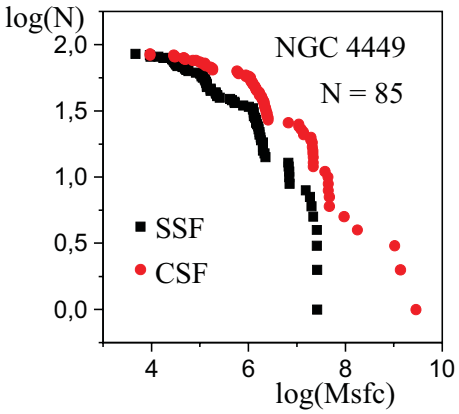

Fig. 6. Mass distribution of 85 star forming regions in the NGC 4449. Square symbols correspond to the instantaneous starburst (SSF). Circles correspond to the case of continuous star formation (CSF).

from our catalogue of $UBVR$ and H_α photometry presented in paper I (Sakhibov & Smirnov 1999). Some individual SFCs in these galaxies belong to the sample of 105 SFCs (last column in Table 4) and were used in the estimation of linear regression Eqs. (16), (17) and (23), (24). We have used the Eqs. (16), (17), (19), (21), (23), (24) to estimate the slope α of IMF and mass M_{SFC} from luminosity M_B to study the mass distribution of SFCs in these galaxies.

The slope, range, mean of the mass, luminosity and size distributions of SFCs in the individual galaxies are indicated in Table 5. Throughout the calculation of M_{SFC} from observed B magnitudes, we have to assume a star formation regime. In the case of star burst galaxies NGC 4038/39 (Genzel et. al. 1997) the choice of regime is clear. It should be noted that the 7 SFCs in the NGC 4038/39 studied in Sect. 5 show instantaneous star burst (SSF model) too. We have displayed in Table 5 both cases of the mass distributions of SFCs. In the case of constant star formation (CSF model), mass spectrum of star forming regions covers the range of higher values of mass (see Fig. 6.).

In Figs. 6 and 7a we have plotted on a logarithmic scale the number of SFCs N with a mass greater than a given value versus the SFC mass M_{SFC}. In Fig. 7b and Fig. 7c the same distributions of luminosity M_B and sizes l (pc) of SFCs are displayed. Fig. 7a shows mass distribution of SFCs (in instantaneous burst approximation) in the five galaxies.

The plotted mass functions in the studied galaxies of different morphological types show a similar form: slope b changes from -0.38 up to -0.63. Some authors studied differential distributions (for example for luminosity function LF) in form $x = d[log(N/\Delta L)]/d[log(L)]$, where slope x can be expressed through slope b of integral distribution as $x = (b - 1)$. The mass function of the SFCs in the studied galaxies is close to the luminosity function of star clusters in LMC with $b = -0.5$ ($x = -1.5$, Elson & Fall 1985). The Galactic molecular cloud masses are also distributed in a similar way, with b = -0.6 (x = -1.6, Williams & McKee 1997).

7. Integral IMF in galaxies

In Sect. 6, throughout the calculations of masses of individual SFCs in galaxies NGC 2403, 2903, 4038/39, 4303, 4449 the

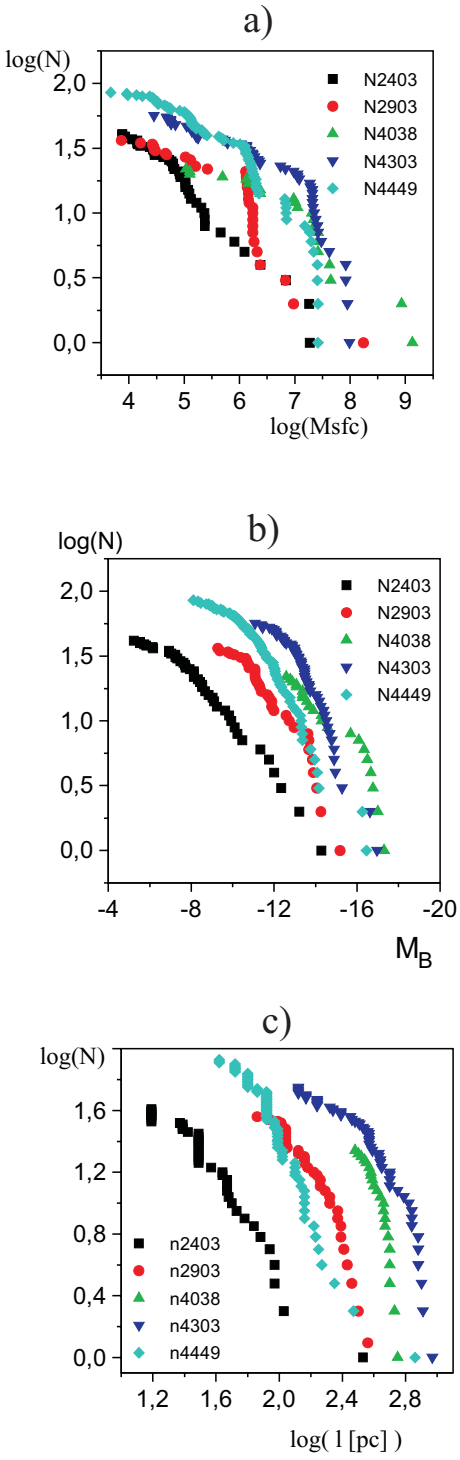

Fig. 7. **a** Mass, **b** luminosity and **c** size functions of SFCs in the studied galaxies.

estimations of slope α, upper mass limit M_{max} and normalising constant A of IMF in all observed SFCs were derived. This gives the possibility to estimate the initial number of stars at fixed mass m in an individual SFC:

$$n_i(m) = A_i m^{\alpha_i} \tag{25}$$

where α_i is the estimated slope of the IMF in the individual SFC, A_i is the value of the normalising constant estimated from Eq. (19). Since the samples of SFCs in these galaxies are mostly complete, we can calculate a total initial number of stars $N(m)$ of fixed mass m in all SFCs in a given galaxy as

$$N(m) = \sum_{i=1}^{N_{SFC}} A_i m^{\alpha_i} \tag{26}$$

where N_{SFC} is the total number of star forming regions in the galaxy. In Fig. 8 we have plotted on a logarithmic scale the calculated total initial number of stars $N(m)$ of mass m versus the stellar mass m (in instantaneous burst approximation) separately for each of the studied galaxies. Because the lower mass end of the IMF is not known from observations and about 80% of the luminosity of SFCs is provided by high mass stars ($m > 4M_\odot$), the integral IMF in a given galaxy is built for the stellar mass interval from $4M_\odot$ to M_{max}. Star forming regions with a low upper mass limit (for example with $M_{max} < 40M_\odot$) do not contribute to the high mass part of the galactic integral IMF. This effect causes the sharp decreasing of the number of high mass stars in the galaxy NGC 2403 (see Fig. 8a). Since the major part of the integral IMF ($m < 60M_\odot$ or in $log(m) < 1.8$) provides more than 90% of the luminosity and contains more than 97% mass of SFCs, we adopted the stellar mass value $m = 60M_\odot$ as upper mass limit of the integral IMF in the galaxy NGC 2403.

Slopes of stellar mass distributions estimated by the least mean square method for five studied galaxies are indicated in Table 6. We have presented both cases: instantaneous burst (SSF model) and continuous star formation (CSF model). Both approximations constrain the slope of the integral IMFs close to Salpeter IMF, despite the broad range of variation of the slope α in individual SFCs from $\alpha = -0.5$ to $\alpha = -4.0$ (see Table 6). The high mass SFCs ($M_{SFC} > 10^6 M_\odot$) provide the major contribution to the integral IMF in a galaxy. Therefore the underestimation of the number of faint SFCs is not important.

We have estimated the star formation rate $\dot{M}$ in a galaxy within the stellar mass interval from $4M_\odot$ to the upper mass limit of the integral IMF M_{max} from the total amount of gas transformed into stars (total stellar mass within the stellar mass interval $4M_\odot - M_{max}$) in all SFCs:

$$M^*_{tot} = A \int_{M_{min}}^{M_{max}} N(m) m^\alpha dm \tag{27}$$

where constant A is estimated from the integral IMF in a galaxy plotted in Fig. 8b. Since the parameters α_i, A_i in formula (26) are related to the IMF of individual SFCs, not to the present stellar mass functions, the value of the total amount of gas transformed into stars (M^*_{tot}) corresponds to the onset of star formation. The total mass M^*_{tot} is computed assuming instantaneous star burst. In the case of continuous star formation the low limit of the total amount of gas transformed into stars and appropriately the low limit of the rate of star formation can be estimated (see Table 6, Column 4). The star formation rate $\dot{M}$ (see Table 6) was derived

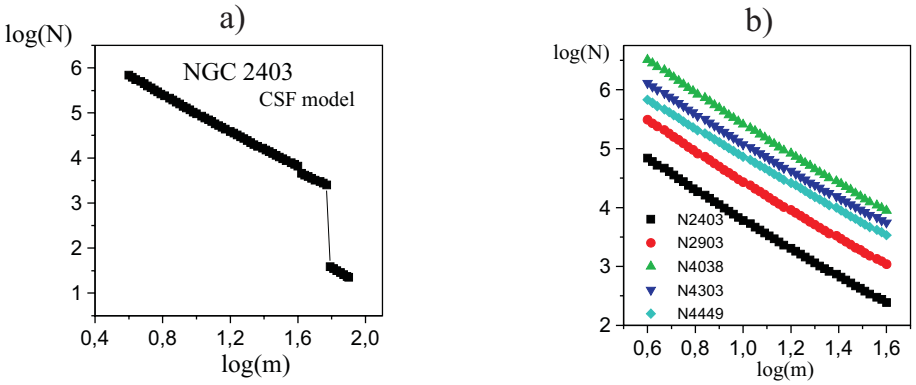

Fig. 8. a Integral stellar IMF in the NGC 2403. The sharp jump down at mass $60M_{\odot}$ is due to the sharp decrease of the number of SFCs with upper mass limit $M_{max} > 60M_{\odot}$. **b** The integral IMFs in the studied galaxies are close to Salpeter IMF($\alpha = -2.35$).

Table 6. IMF, rate of star formation, SN frequency in studied galaxies.

NGC	Integral IMF slope α		M_{max} $[M_{\odot}]$		SFR $[M_{\odot}/yr]$		SFR from FIR fluxes $[M_{\odot}/yr]$	SN frequency $1/\tau$ τ [yr]	
1	2		3		4		5	6	
	SSF	CSF	SSF	CSF	SSF	CSF		SSF	CSF
2403	-2.46	-2.06	40	60	0.29	> 4.4	0.4	125	< 8
2903	-2.45	-2.37	40	60	0.83	> 5.5	2.8	45	< 7
4038/39	-2.57	-2.17	40	60	36			3	
4303	-2.57	-2.20	80	40	2.5	> 69	2.2	20	< 0.5
4449	-2.30	-2.30	40	40	2			20	

from the estimated M^*_{tot} and average age of SFCs $\bar{t}$ in a given galaxy:

$$\dot{M}[M_{\odot}/yr] = M^*_{tot}/\bar{t} \tag{28}$$

Star formation rate (SFR) from observed FIR flux L_{FIR} is computed using the above estimated above slope of integral IMF, and mean age of SFCs $\bar{t}$ of a given galaxy:

$$\dot{M}_{FIR}[M_{\odot}/yr] = (1/\bar{t}) \left(\frac{\overline{M}}{\overline{L}}\right) L_{FIR} \tag{29}$$

where

$$\overline{M} = \frac{\int\limits_{M_{min}}^{M_{max}} m \cdot m^{\alpha} dm}{\int\limits_{M_{min}}^{M_{max}} m^{\alpha} dm} \tag{30}$$

and

$$\overline{L} = \frac{\int\limits_{M_{min}}^{M_{max}} L^*(m) m^{\alpha} dm}{\int\limits_{M_{min}}^{M_{max}} m^{\alpha} dm} \tag{31}$$

We assumed that the observed FIR luminosity accounts for the bolometric luminosity of all stars borne in all SFCs in the parent galaxy. Comparison between estimation of SFR from integral IMF (Column 4 in Table 6) and that from observed FIR luminosity can constrain the regime of star formation into the benefit of instantaneous burst in NGC 2403, 2903, 4303.

We also estimated the SN frequency $(1/\tau)$ in these galaxies as a number of formed stars with mass greater then $10M_{\odot}$ per year (see Table 6, Column 6). In the case of continuous star formation model estimations of τ are the upper limit of intervals between SN events. The observed average interval τ_{obs} between successive supernovae in NGC 4303 (Flin et al. 1979) is 19 years and the interval τ_{radio} computed from the radio fluxes of NGC 4303 is 13 years (Smirnov & Sakhibov 1984). These two values are close to the interval τ estimated assuming instantaneous burst in NGC 4303. The observed average interval τ_{obs} between SN in NGC 4038/39 is about 50 years (Flin et al. 1979). The detection of the frequent SN calculated for this starburst galaxy could be hidden by very large light absorption.

The estimated star formation rate $\dot{M}$ for the three spirals (NGC2403, NGC2903, NGC4303) and the one irregular (NGC4449) galaxy are in good agreement with evolution models of galaxies (Samland & Hensler 1996) and IRAS observations (Sage 1993; Soifer et al. 1989).

Peculiar colliding galaxy NGC4038/39 shows the highest star formation rate. Apparently the burst of star formation is caused by interaction of two galaxies. The mid-infrared spectroscopic observations of the interacting galaxies NGC 4038/39 obtained with the ISO Short Wavelength Spectrometer are well described by star burst models for a recent star burst with an initial mass function extending up to 100 Solar Masses (Genzel et al. 1997). This is an observational confirmation of our estimation of a very high rate of star formation and high SN frequency.

Table 7. Relationship between the IMF slope α and SFC mass.

M_{SFC} $[M_\odot]$	10^3	10^4	10^5	10^6	10^7	10^8	10^9
α	-1.0	-1.35	-1.70	-2.05	-2.40	-2.75	-3.1

8. Discussion

The important result from this work is that the star formation parameters derived for the sample of 105 SFCs are in a good agreement with the results of the study of star formation bursts in 17 star forming regions by Mas-Hesse & Kunth (1999) using different methods. We found no correlation between the chemical abundance Z and the IMF parameters (slope α and upper mass limit M_{max}). The same conclusion is made from the study of star formation bursts in irregular and compact galaxies by Mas-Hesse & Kunth (1999). They suggested that it is not necessary to propose the trend toward flatter IMFs at low metallicities to explain the correlation toward higher values of the effective temperature $W(H_\beta)$ values at low metallicities.

The upper cut-off sizes of SFCs in a galaxy are determined by the thickness of the disk ($\sim 0.5-1kpc$). Large and intermediate size SFCs have high star density ($> 0.25 M_\odot pc^{-3}$). Small SFCs have a star density close to the gas density in the solar neighbourhood ($\sim 0.02 M_\odot pc^{-3}$). It seems that the lower cut-off of SFC density determines the lower cut-off of SFC mass and size. From the models of evolution of galaxies it is well known that the disk thickness and gas density are dependent on the stage of evolution and type of galaxy (Samland & Hensler 1996). This implies the existence of different upper and lower cut-offs of the mass function of SFCs in different galaxies.

In Table 7 we have listed the relation (22) between slope α of IMF and mass of star forming region M_{SFC} discussed above in Sects. 5 and 6. From Table 7 one can see that the slope of IMF increases with the mass of individual SFC: IMF of small, low mass SFC is flatter than Salpeter IMF; IMF of intermediate SFC is close to Salpeter slope $\alpha = -2.35$; and IMF of large, high mass SFC is steeper than Salpeter one. Since the characteristic ranges of M_{SFC} in the studied galaxies are from $10^4 M_\odot$ to $10^8 M_\odot$, the ranges of slopes α cover the interval from $\alpha \approx -1$ to $\alpha \approx -3$ The Salpeter slope $\alpha = -2.35$ is located near the centre of the range of slope's variation. Such ranges of the mass distribution functions of SFCs provide the forms of the integral IMFs very close to Salpeter IMF in the studied galaxies. When the upper cut-off of the mass function of SFCs is lower than $10^6 M_\odot$ we can expect the integral IMF in galaxies to be flatter than Salpeter IMF.

In conclusion we can say that the range of variation of the star formation properties of SFCs in galaxies is determined by the range of the mass distribution function of star forming regions, while the integral stellar IMF in galaxies stands close to Salpeter IMF. The changes in star formation properties in different galaxies are related to the changes in individual SFCs mass functions and the correlation of the IMF in individual SFCs with the mass of SFC.

Acknowledgements. We are grateful to V.I. Myakutin and A.E. Piskunov for providing us with their synthesis models and fruitful cooperation. We wish to thank our referee J.M. Mas-Hesse for his comments and recommendations which significantly improved the paper. Part of this work was supported by the Russian Fund for Fundamental Investigation (RFFI), project code 95-02-04260.

References

Allen C.W., 1973, Astrophysical quantities. University of London, Athlone Press
Avedisova V.S., 1979, AZh 56, 965
Bica E., Alloin D., Schmidt A., 1990, MNRAS 242, 241
Bresolin F., Kennicutt R., 1997, AJ 113, 975
Caplan J., Deharveng L., 1986, A&A 155, 297
Charbonnel C., Meynet G., Maeder A., Schaller G., Schaller D., 1993, A&AS 101, 415
Charbonnel C., Meynet G., Maeder A., Schaller G., Schaller D., 1993a, A&AS 102, 339
Charbonnel C., Meynet G., Maeder A., Schaller G., Schaller D., 1994, A&AS 103, 97
de Vaucouleurs G., de Vaucouleurs A., Corwin Jr. H.G., 1976, Second Reference Catalogue of Bright Galaxies. University of Texas Press, Austin
Dobrodiy S.A., Pronik I.I., 1979, Izvestia Cryimskoi Astrofizicheskoi Observatorii 60, 66
D'Odorico S., Rosa M., Wampler E.J., 1983, A&AS 53, 97
Elson R.A.W., Fall M., 1985, PASP 97, 692
Flin P, Karpowicz M., Murawski W., Rudnicki K., 1979, Catalog of Supernovar. Acta Cosmol. No 8, 5, Circ. IAU 3348, 3542
Genzel R., Lutz, D., Egami E., et al., 1997, Rev. Mex. Astron. Astrofis. Ser. Conf. 6, 7
Grigorieva N.B., 1976, Izvestia Cryimskoi Astrofizicheskoi Oservatorii, 54, 171
Grigorieva N.B., 1979, Izvestia Cryimskoi Astrofizicheskoi Observatorii 59, 188
Grigorieva N.B., 1980, Izvestia Cryimskoi Astrofizicheskoi Observatorii 62, 39
Johnson H.L., 1966, ARA&A 4, 193
Khachikian E.Ye., Sahakian K.A., 1970, Afz 6, 177
Leitherer C., Heckman T., 1995, ApJS 96, 9L
Lequeuex J., Maucherat-Joubert M., Deharveng J.M., Kunth D., 1981, A&A 103, 305
Maiz-Apellaniz J., Mas-Hesse J.M., Munoz-Tunon C., Vilchez J.M., Castaneda H.O., 1998, A&A 329, 409
Mas-Hesse J.M., Kunth D., 1991, A&AS 88, 399
Mas-Hesse J.M., Kunth D., 1999, A&A 349, 765
Mayya Y.D., 1994, A&A 108, 127
McCall M.L., Rybski P.M., Shields G.A., 1985, ApJS 57, 1
Mezger P.O., 1978, A&A 70, 565
Myakutin V.I., 1992, Astonomiceskij Circular No. 1553, 15
Myakutin V.I., 1995, private communication
Myakutin V.I., Piskunov A.E., Sakhibov F., Smirnov M.A., 1994, In: Astron. Posters Abstracts. XXIInd General Assembly of IAU, p. 59
Olofsson K., 1989, A&AS 80, 317
Piskunov A.E., Myakutin V.I., 1996, AZh 73, 520
Pronik I.I., 1972, Izvestia Crymskoi Astrofizicheskoi Observatorii 45, 162
Pronik I.I., Chuvaev K.K., 1967, Izvestia Crymskoi Astrofizicheskoi Observatorii 38, 219

Pronik I.I., Chuvaev K.K., 1969, Izvestia Crymskoi Astrofizicheskoi Observatorii 40, 96
Pronik I.I., Chuvaev K.K., 1971, Izvestia Crymskoi Astrofizicheskoi Observatorii 43, 101
Pronik I.I., Chuvaev K.K., 1972, Izvestia Cryimskoi Astrofizicheskoi Observatorii 44, 40
Sagar R., Piskunov A.E., Myakutin V.I., Joshi U.C., 1986, MNRAS 220, 383
Sage L.J., 1993, A&A 272, 123
Sakhibov F., Smirnov M.A., 1990, AZh 67, 472
Sakhibov F., Smirnov M.A., 1995, AZh 72, 318
Sakhibov F., Smirnov M.A., 1999, AZh accepted (Paper I)
Sakhibov F., Smirnov M.A., 1999a, AZh submitted (Paper II)
Smirnov M.A., Sakhibov F., 1984, SvA 28, 137
Samland M., Hensler G., 1996, Proc. IAU Symp. 171, p. 23
Scalo J., 1986, Fundamentals of Cosmic Physics 11, 1
Schaller G., Schaller D., Meynet G., Maeder A., 1992, A&AS 96, 269
Schaller G., Schaller D., Meynet G., Maeder A., 1993, A&AS 98, 523
Schmidt-Kaler Th., 1982, Landolt-Bernstein Numerical Data and Functional Relationships in Science and Technology. Vol.2 Springer, Berlin-Heidelberg, p. 15; 453
Shahbazian R.K., 1970, Afz 6, 367
Shapovalova A.I., 1971, Vestnik Kievskogo Universiteta, ser. str. N 13, 104
Smith L.F., Mezger P.G., Biermann P., 1978, A&A 66, 65
Soifer B.T., Boehmer L., Neugebauer G., Sanders D.B., 1989, AJ 98, 766
Terlevich R., Melnick J., 1985, MNRAS 213, 841
Vilchez J.M., Pagel B.E.J., 1988, MNRAS 231, 257
Williams J.P., McKee C.F., 1997, ApJ 476, 166
Zaritsky D., Kennicutt R. C., Huchra J.P., 1994, ApJ 420, 87